

tential used by Kloet and Tjon,⁸ which has a soft repulsive core, we find the phase shift ${}^4\delta_0 = 68^\circ$ and absorption coefficient ${}^4\eta_0 = 0.97$ at $E_{lab} = 14.1$ MeV, to be compared with the results ${}^4\delta_0 = 72.5^\circ$ and ${}^4\eta_0 = 0.975$ obtained in Ref. 8. At $E_{lab} = 46.3$ MeV we find ${}^4\delta_0 = 35^\circ$, ${}^4\eta_0 = 0.90$, compared to 38.7° and 0.883 . At $E_{lab} = 3.27$ MeV our results were unstable, possibly because of threshold effects which will require special treatment. In view of the present state of the three-body scattering problem and the fundamental differences of the methods in Refs. 6 and 8, we find this general agreement rather promising.

Our above-described approach has the advantage of providing a direct solution to the problem, thus being free from any convergence consideration. The discretization problem which remains arises anyway with all other methods. The direct solution is made possible by the use of configuration space since the local nature of differential operators (compared with integral operators) makes the rank of matrices we have to handle an order of magnitude smaller than for the direct solution of Faddeev integral equations. Moreover the use of configuration space gets rid of any singularities usually associated with the momentum-space integral equations. The practical advantages of this method are similar to

those that the Schrödinger equation has over the Lippmann-Schwinger equation. Finally we are here faced with the preliminary problem of building the two-body bound-state wave function rather than the two-body t matrix occurring in the integral equations, which is much easier for the same reasons. Taking advantage of the great simplicity and efficiency of this method, we are presently dealing with the realistic problem of three-nucleon scattering with a tensor force.

¹L. D. Faddeev, Zh. Eksp. Teor. Fiz. **39**, 1459 (1960) [Sov. Phys. JETP **12**, 1014 (1961)], and *Mathematical Aspects of the Three-Body Problem in Quantum Theory* (Israel Program for Scientific Translations, Jerusalem, 1965).

²J. Nuttall, Phys. Rev. Lett. **19**, 473 (1967).

³S. P. Merkuriev, Laboratoire de Physique Théorique et Haute Energies Report No. 74/1 (to be published).

⁴S. P. Merkuriev, G. Gignoux, and A. Laverne, to be published.

⁵A. Laverne and G. Gignoux, Nucl. Phys. **A203**, 597 (1973).

⁶J. Revai and J. Raynal, Lett. Nuovo Cimento **9**, 461 (1974).

⁷It was pointed out to us by W. Glöckle that x small makes $A = \psi/\varphi \exp(iqy)$ to order $y^{-3/2}$.

⁸W. M. Kloet and J. A. Tjon, Ann. Phys. (New York) **79**, 407 (1973).

Single-Pion Production at 100 GeV/c: A Detailed Test of Factorization

J. Erwin, Winston Ko, R. L. Lander, D. E. Pellett, and P. M. Yager
*Department of Physics, University of California, Davis, California 95616**

and

M. Alston-Garnjost
Lawrence Berkeley Laboratory, University of California, Berkeley, California 94720†
(Received 19 August 1974)

A relatively bias-free comparison is made of inclusive and semi-inclusive charged-pion single-particle spectra in π^+p and pp interactions. Inclusive Mueller factorization is satisfied by π^- but not π^+ production. Factorization holds for proton-target fragmentation into π^- for a fixed number of π^- backward in the c.m. system, but not for fixed total multiplicity. In the central region, $\pi^+p \rightarrow \pi^+$ shows an $s^{-1/4}$ approach to the same value, ~ 0.78 , seen in other reactions.

We report results of an exposure of the Fermi National Accelerator Laboratory 30-in. hydrogen bubble chamber to an unseparated but tagged π^+ and p beam at 100 GeV/c. The mixed beam allows comparison of the secondary pion spectra from high-energy π^+p and pp collisions with mini-

num biases, providing an excellent test of factorization: independence of secondary spectra from the identity of the incident projectile.

While factorization is an important experimental matter in itself, it is of particular interest and perhaps crucial to Mueller-Regge theory.

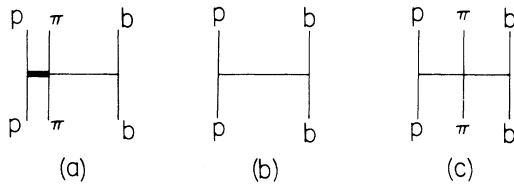


FIG. 1. Mueller diagrams for (a) pion production in the proton fragmentation region, (b) total cross section, and (c) pion production in the central region.

Here, the inclusive cross section for pions in the fragmentation region can be represented by the Mueller diagram in Fig. 1(a). If the Pomeron dominates the link between the beam (particle b in Fig. 1) and the πp "blob," and if it is factorizable, the cross section can be written¹⁻³ in the form of a product,

$$d^2\sigma/dy dp_T^2 = \beta_{\pi p}(y, p_T^2)\beta_b. \quad (1)$$

This result is analogous to the factorization of the total cross section indicated by the Mueller diagram in Fig. 1(b):

$$\sigma_T = \beta_p\beta_b. \quad (2)$$

When we divide Eq. (1) by (2), the quantity

$$(\sigma_T)^{-1}d^2\sigma/dy dp_T^2 = \beta_{\pi p}(y, p_T^2)/\beta_p \quad (3)$$

becomes independent of projectile identity. At finite energies, Reggeon contributions to the diagram of Fig. 1(a) require another term in Eq. (1):

$$\frac{d^2\sigma}{dy dp_T^2} = \beta_{\pi p}(y, p_T^2)\beta_b + \beta_{\pi p}'(y, p_T^2)\beta_b's^{-1/2}. \quad (4)$$

The quantity $(\sigma_T)^{-1}d^2\sigma/dy dp_T^2$ now approaches factorization like $s^{-1/2}$.

In the central region, where y is small, we can write the inclusive distribution according to Fig. 1(c). If the Pomeron dominates both exchange links, we have

$$d^2\sigma/dy dp_T^2 = \beta_p\beta_b\gamma(p_T^2). \quad (5)$$

The height at the center of the distribution $(\sigma_T)^{-1}d^2\sigma/dy dp_T^2 = \gamma(p_T^2)$ is then independent of both target and beam. There is an $s^{-1/4}$ approach to this limit from the additional term² to Eq. (5) that is necessary when Reggeons are included in the exchanges,

$$\frac{d^2\sigma}{dy dp_T^2} = \beta_p\beta_b\gamma(p_T^2) + (\beta_p'\beta_b + \beta_p\beta_b')\gamma'(p_T^2)(\sqrt{s})^{-1/2}. \quad (6)$$

In this experiment,⁴ secondary pion distributions, $\rho = (\sigma_T)^{-1}d\sigma/dy$, were obtained under identical conditions for two different projectiles, π^+ and p . The $\pi^+:p$ ratio in the unseparated beam was about 7:8. The identity of each incident particle was determined by a 35-m differential Cherenkov counter used in conjunction with three sets of multiwire proportional chambers. π^+p and pp events were treated identically in the scanning and measuring process. Errors due to absolute-cross-section normalization were avoided through use of the relation

$$\rho = \frac{1}{\sigma_T} \frac{d\sigma}{dy} = \frac{1}{N_T} \frac{dN}{dy}, \quad (7)$$

where N_T is the total number of events in the data sample corrected for two-prong scanning inefficiency. The experiment thus provides a test of factorization with systematic errors minimized.

All events were measured on a Lawrence Berkeley Laboratory spiral reader with automatic track matching. Using the known forward-backward symmetry in the c.m. system for pp interactions, we can determine the efficiency for track reconstruction separately for each topology in the backward and forward hemispheres of the c.m. system. These efficiencies can then be applied to the π^+p samples. Reconstruction efficiency for tracks in the backward hemisphere was better than 96% independent of multiplicity. In the forward hemisphere, the efficiency dropped with increasing multiplicity, with 80% of the tracks reconstructed on the average. The number of tracks from π^+p events, computed after weighting with efficiencies obtained from pp interactions, was consistent with the number obtained in the scan count. This agreement held for each topology separately. Track-reconstruction losses thus appear to be identical for pp and π^+p events.

To compare spectra for secondary particles from π^+p and pp interactions, it is most appropriate to take the ratio of single-particle spectra, for then the efficiency factor will divide out. We find (see Fig. 2) that for π^- , the ratio

$$\frac{\rho_-(\pi^+p)}{\rho_-(pp)} = \frac{(\sigma_T)^{-1}d\sigma(\pi^+p \rightarrow \pi^-)/dy}{(\sigma_T)^{-1}d\sigma(pp \rightarrow \pi^-)/dy} \quad (8)$$

is flat and almost 1 in the backward hemisphere in the c.m. system up to $y = -0.6$.⁵ The ratio for all events with $y < -0.6$ is 0.98 ± 0.04 . Factorization in this region thus works remarkably well for π^- . We note that the ratio in the forward hemisphere rises approximately linearly. This ratio measures the difference in the structure

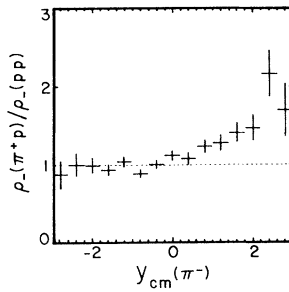


FIG. 2. Ratio of $(\sigma_T)^{-1}d\sigma/dy$ for π^- produced in π^+p and pp interactions.

functions of the two projectiles.

The fact that the ratio is a constant and consistent with unity in the backward hemisphere shows that, at 100 GeV/c and within the framework of the theory, the Pomeron dominates the process of Fig. 1(a) and Pomeron factorization is satisfied to within a few percent. That is, the function $\beta_{\pi p}(y, p_T^2)$ in Eq. (3) has the same y dependence in π^+p and pp interactions. In Fig. 3(a) we make a comparison of the p_T distributions for events in the backward hemisphere. The ratio is again consistent with 1 for all p_T . Furthermore, when we compare in Fig. 3(b) the average p_T as a function of y for these same two reactions, we see that they are nearly the same at any value of y in the backward hemisphere. Our conclusion is therefore that, in the inclusive reactions $\pi^+p \rightarrow \pi^-$ and $pp \rightarrow \pi^-$, factorization works; $\beta_{\pi p}(y, p_T^2)$ is independent of the projectile.

As we examine further the details of factorization, Fig. 4(a) shows that the ratio of Eq. (8) at a fixed charged-particle multiplicity is *not* 1, or even a constant, at all multiplicities. The Mueller picture does not make any prediction about these ratios. However, if target fragmentation is indeed independent of the projectile, then the ratio of Eq. (8) in the target fragmentation region should be the same for π^+ and p projectiles for a fixed multiplicity over that region. This "proton fragmentation multiplicity" cannot be known, since neutrals are not observed. We may approximate it by selecting a fixed number of π^- in the backward hemisphere. These selections are shown in Fig. 4(b). The ratios are constant and have a value consistent with unity in the backward hemisphere.

It is indeed quite remarkable that factorization works in such detail. There were indications of factorization at lower energies for the π^- fragments of the proton.⁶ The agreement was usually

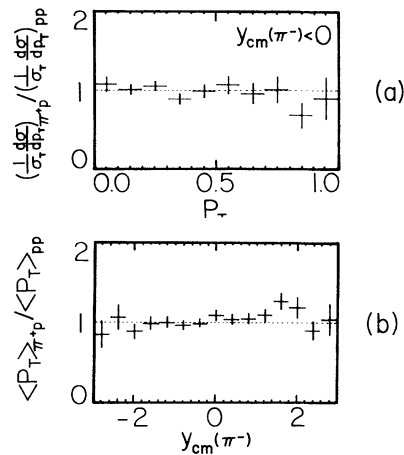


FIG. 3. (a) Ratio of $(\sigma_T)^{-1}d\sigma/dp_T$ for π^- produced backward in the c.m. system in π^+p and pp interactions. (b) Ratio of average P_T for π^- produced in π^+p and pp interactions as a function of y .

good to 10%. Mueller's picture with a factorizable Pomeron will give exact factorization. Some recent work on a geometric model⁷ can also give approximate factorization to 10%. The degree of

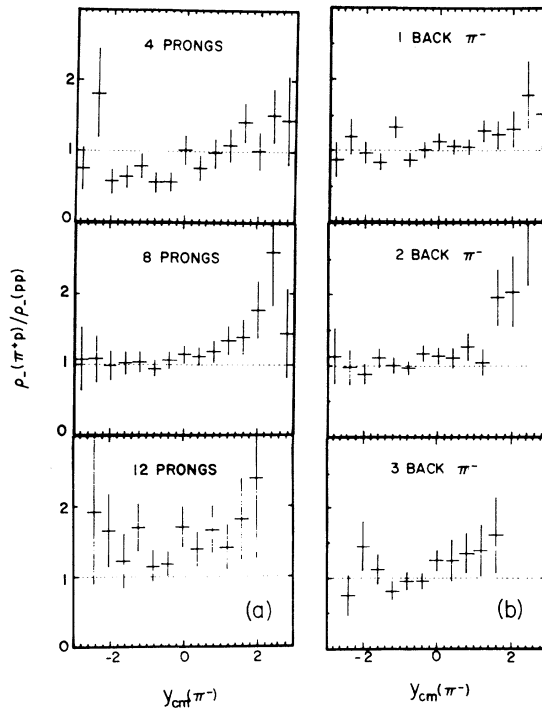


FIG. 4. (a) Ratio of $(\sigma_T)^{-1}d\sigma/dy$ for π^- produced in π^+p and pp interactions at given multiplicities. (b) Ratio of $(\sigma_T)^{-1}d\sigma/dy$ for π^- produced in π^+p and pp interactions at given π^- multiplicity in the backward hemisphere.

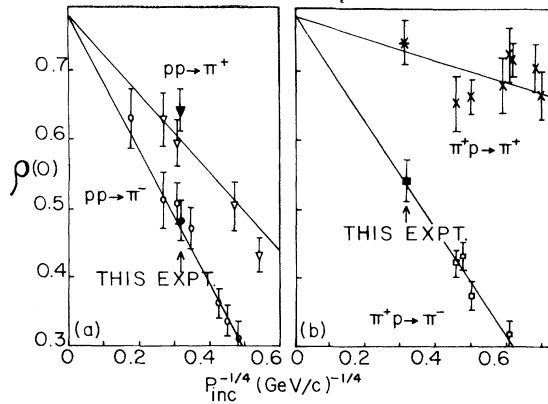


FIG. 5. $(\sigma_T)^{-1}d\sigma/dy|_{y=0}$ for pions produced (a) in pp interactions and (b) in π^+p interactions.

factorization we have observed makes the Mueller picture look very good.

In the central region, $y_{c.m.}=0$, factorization says that pion production is independent of both target and projectile. The density function, Eq. (7), is then independent of incident energy. As indicated in Eq. (6), there is an $s^{-1/4}$ approach to factorization in the central region. In Figs. 5(a) and 5(b) the values of ρ at $y_{c.m.}=0$ for charged-pion production in pp and π^+p reactions are plotted as a function of $P_{inc}^{-1/4}$. The extrapolation to $s = \infty$ is indeed consistent with (although does not compel) the hypothesis that *all* curves approach a single point.⁸ In other words, from Eq. (5), at $s = \infty$ and $y_{c.m.}=0$,

$$\rho = \int \gamma(p_T^2) dp_T^2 \quad (9)$$

is a constant independent of projectile.

We note from Figs. 5(a) and 5(b) that the π^+ produced in the π^+p interaction are more numerous than those in the pp interaction relative to their respective total cross sections. Now if we look at the ratio

$$\frac{\rho_+(\pi^+p)}{\rho_+(pp)} = \frac{(\sigma_T)^{-1}d\sigma(\pi^+p \rightarrow \pi^+)/dy}{(\sigma_T)^{-1}d\sigma(pp \rightarrow \pi^+)/dy}, \quad (10)$$

we see in Fig. 6(a) that even in the target fragmentation region this excess persists. However, the ratio is still quite constant in y . Furthermore as shown in Fig. 6(b), the ratio between the average p_T of the π^+ , like that of the π^- , is the same for all y in the π^+p and pp interactions. For π^+ production, factorization even in the fragmentation region is not achieved yet at 100 GeV/c, but the structure functions, $\beta_{\pi p}(y, p_T^2)$ and $\beta_{\pi p}'(y, p_T^2)$ in Eq. (4), seem to have the same y and p_T^2 de-

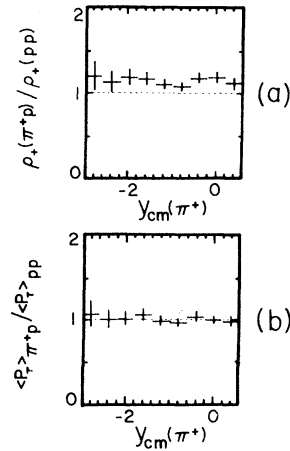


FIG. 6. (a) Ratio of $(\sigma_T)^{-1}d\sigma/dy$ for π^+ produced in π^+p and pp interactions. (b) Ratio of average p_T for π^+ produced in π^+p and pp interactions as a function of y .

pendence.

In conclusion, we note a regularity in the data related to exoticity.⁹ Using the notation $b+a \rightarrow c+X$, we may ask which of the combinations $abc\bar{c}$, $a\bar{c}$, $b\bar{c}$, and ab are exotic for each reaction. We find that the two reactions $\pi^+p \rightarrow \pi^-X$ and $pp \rightarrow \pi^-X$ are simultaneously exotic only in $abc\bar{c}$, and these are the reactions for which factorization is satisfied. The other two reactions are simultaneously exotic in none of the above combinations, and factorization fails by $\sim 13\%$ for these reactions. This result suggests that if exoticity plays any part at all, it is $abc\bar{c}$ exoticity that operates.

The cooperation of the Fermi National Accelerator Laboratory and in particular the neutrino laboratory personnel is acknowledged with pleasure. The multiwire-proportional-chamber tagging system was designed and built by the Proportional Hybrid System Consortium. We would like to thank them for its use and for their help in operating it. We would like also to thank W. R. Frazer and L. S. Brown for fruitful conversations.

*Work supported in part by the U. S. Atomic Energy Commission under Contract No. AT(04-3)-34 PA 191.

†Work done under the auspices of the U.S. Atomic Energy Commission.

¹A. H. Mueller, Phys. Rev. D 2, 2963 (1970).

²H. D. I. Abarbanel, Phys. Lett. 34B, 69 (1971).

³For a review of the subject see also D. Horn and F. Zachariasen, *Hadron Physics at High Energies* (Benjamin, New York, 1973). We follow the notation of this

reference.

⁴J. Erwin *et al.*, Phys. Rev. Lett. **32**, 254 (1974).

⁵The limit -0.6 is chosen in order that the data lie within 2 units of rapidity of the target.

⁶For a summary of previous experimental work, see R. Lander, in *Particles and Fields—1971*, edited by A. C. Melissinos and P. F. Slattery, AIP Conference Proceedings No. 2 (American Institute of Physics, New York, 1971), p. 71.

⁷H. Cheng, J. K. Walker, and T. T. Wu, Phys. Rev. D **9**, 749 (1974).

⁸L. S. Brown, Phys. Rev. D **4**, 2760 (1971); M. Alston-Garnjost, in *Proceedings of the International Conference on Inclusive Reactions*, Davis, California, 1972, edited by R. L. Lander (Univ. of California, Davis, California, 1972), p. 182; M. Alston-Garnjost *et al.*, Phys. Lett. **39B**, 402 (1972); T. Ferbel, Phys. Rev. Lett. **29**, 448 (1972).

⁹Chan H.-M., C. S. Hsue, C. Quigg, and J. M. Wang, Phys. Rev. Lett. **26**, 672 (1971); J. Ellis, J. Finkelstein, P. H. Frampton, and M. Jacob, CERN Report No. TH 1216, 1971 (to be published).

COMMENTS

Dynamic Properties of a Nonsuperfluid Bose Liquid in the Random-Phase Approximation

S. W. Lovesey

Institut Laue-Langevin, 38042 Grenoble, France

and

D. C. Mattis and L. F. Landovitz

Belfer Graduate School of Science, Yeshiva University, New York, New York 10033

(Received 26 June 1974)

The dynamic structure factor $S(k, \omega)$ of a nonideal Bose liquid is calculated within the random-phase approximation and compared with neutron scattering data by Cowley and Woods for liquid helium in the temperature range $T_\lambda < T \leq 4.2^\circ\text{K}$, with the conclusion that the model is wholly inadequate. A low-frequency pole in the generalized susceptibility discussed by Mattis and Landovitz is shown to be overdamped in $S(k, \omega)$.

In studying the poles of the dynamic structure factor $S(k, \omega)$ for He^4 above the X point, Mattis and Landovitz in an earlier Letter¹ concluded that not one but *two* modes of wave propagation comprised the normal modes of the system, and that the speed of propagation s of one of them fitted a law

$$s \propto (T - T_\lambda)^{1/2}$$

near T_λ , whereas the speed of the other was fairly insensitive to temperature.

In subsequent numerical work on the width of the resonances identified as these normal modes, we discovered that the widths were such that, in fact, only a single mode could be perceived, in contradiction to our earlier results. We then attempted to fit the parameters to the neutron data reported by Cowley and Woods² in the temperature range $T_\lambda < T \leq 4.2^\circ\text{K}$. The most striking feature of these data is that the energy and lifetime

of the well-defined collective mode observed at 1.1°K , and wave vectors $k \sim 0.2 \text{ \AA}^{-1}$, do not change appreciably on going from He II to He I. We find that the observed temperature dependence of the collective-mode energy is markedly different from that of the collective, random-phase-approximation (RPA) mode in the nonideal Bose liquid; nor does the wave-vector dependence of the observed mode agree with that calculated. Not surprisingly, the widths of the calculated mode are typically a factor of 50 smaller than observed values.

Our calculation is tantamount to an elaboration of ideas originally put forward by Pines³ which exploit the analogy between the collective mode and plasmons in an electron gas. The mode results from the short-range, rather than the long-range, correlations in the liquid, and resembles the zero-sound mode proposed by Landau for Fermi fluids. Pursuing this analogy within RPA leads to an expression for the generalized sus-